4

Stacked Array Antenna with 2-D Beam Switching and Quad-Polarization Reconfigurability

This chapter presents a multifunctional stacked array antenna with 2-D beam switching and quad-polarization reconfigurability for 5G sub-6GHz applications. Four different polarization states (vertical polarization (VP), horizontal polarization (HP), left-hand circular polarization (LHCP), and right-hand circular polarization (RHCP)) are accomplished by using a 2-bit polarization tuner. The beam switching is realized by integrating a tunable phase feed network. Initially, a single antenna element with three switchable feed probes for 2-bit polarization switching is designed, and then a PIN diode-loaded tunable phase shifter is integrated with the feed structure of the 2×2 array for beam switching. By using the different coding sequences of each radiating element, the radiation beam and polarization of the array can be arbitrarily controlled using the single antenna aperture. To demonstrate the proposed concept, a four-element planar array antenna is implemented. Simulation and measurement results ensure that the beam can be switched from -28° to +28° and having the overlapped -10 dB impedance and 3 dB axial ratio bandwidths of 28.5 % (3.5 – 4.7 GHz) and 13 % (3.6 – 4.1 GHz) respectively for all states. Additionally, the proposed antenna has 36 different radiation modes with nine radiation beams and four polarization types for each radiation beam.

4.1 Introduction

Polarization reconfigurable antennas provide radiations of different polarizations by properly utilizing the switching mechanism. These antennas are preferable for high-performance modern wireless communication systems due to their capability of reusing frequency spectrum [148], avoiding polarization mismatch [149], and eliminating multipath fading [150]. Polarization reconfigurable antennas are utilized for a variety of wireless communication applications, for example, satellite communication systems, wireless local area networks (WLAN), and adaptive multiple output multiple input (MIMO) systems. The number of polarizations that an antenna can provide is an important measure of the performance of a polarization reconfigurable antenna. Therefore, the reconfigurable antennas with full polarization, i.e., two orthogonal linear polarizations and two circular polarizations, are highly desirable. Hence reconfigurability in polarization provides an additional degree of freedom in increasing the diversity and capacity of the system. Several literatures have been reported on quad polarization reconfigurable antennas [151], [73], [152]. On the other hand, the beam scanning antennas show multiple radiation modes, beam scanning capability, and beam switching function [92]-[122]. Besides, as compared to one 1-D beam switching, 2-D beam steering provides larger radiation coverage with improved multipath effect and channel capacity [153]. Therefore, the design of a full polarization reconfigurable antenna with 2-D beam steering is of great interest among antenna designers.

With the rapid development of communication technology, multi-parameter reconfigurable antennas are more desirable due to their ability to provide more flexibility and diversity. However, it is extremely difficult to realize a reconfigurable antenna with frequency, polarization, and pattern simultaneously. Also, the realization of a 2-D beam scanning (in the elevation plane) with reconfiguring all four polarization states from a single antenna structure is also difficult. Recently some literature with flexible beam and

reconfigurable polarization have been reported [83], [144], [145], [154]-[156]. Such as, in [83], a corner truncated patch antenna element loaded with four PIN diodes forming a 2×2 array is used to realize a 2-D beam steering with dual circular polarization using the spatial phase shift technique. However, linear polarization is still not realized. In [154], three polarization states, including one Linear Polarization (LP) and two (CP), are attained using a cavity-backed magneto-electric dipole antenna with a ±40° beam scanning range. In [155], a 2-bit polarization reconfigurable antenna with a 1-bit phase shifter (0° and 180°) is designed using a 1x4 linear digitally modulated array. The designed antenna can realize sixteen reconfigurable modes, including four dual beam patterns of each polarization state. Although, the aforementioned antennas can realize pattern reconfigurability with different polarization states simultaneously. However, up to now, an efficient design of 2-D beam switching with reconfigurable quad polarization, including vertical polarization (VP), horizontal polarization (HP), left hand circular polarization (LHCP), and right hand circular polarization (RHCP) has not been reported yet.

In this chapter, the design of 2-D beam switching with four polarization states, including VP, HP, LHCP, and RHCP is presented. By integrating a 2-bit polarization tuner with a designed 2-bit reconfigurable phase variable feed network, the proposed antenna is realized with ability to steer its radiation beam from -28° to +28° and switching its polarization among HP, VP, RHCP, and LHCP simultaneously. Besides, the proposed antenna can realize 36 radiation modes having an overlapped operating bandwidth of 13%, covering the frequency range of 3.6 GHz to 4.1 GHz for both $S_{11} < -10$ dB and AR < 3 dB.

Further, the article is organized in the following manner. Section 4.2 depicts the design and working mechanism of the 2×2 array antenna. Both the simulated and measured results are discussed in section 4.3 for a comparison of different patterns and polarization states. Finally, the comparison of the proposed work with similar existing work and conclusions are drawn in sections 4.4 and 4.5, respectively.

4.2 Reconfigurable Array Design and Working Mechanism

4.2.1 Design of a Quad Polarized Antenna Element

The geometrical structure of the proposed polarization reconfigurable antenna is shown in Fig. 4.1. It is designed using three FR4 substrates (dielectric constant ε_r = 4.4 and a loss tangent tanδ = 0.02) of thickness h. The antenna element mainly consists of three layers, including a parasitic patch layer, a driven patch layer, and a feed network layer. The driven patch layer, placed on the top of the middle substrate, consists of a rectangular patch of length L_1 and width W_1 with three feed probes, as shown in Fig. 4.1(b). To enhance the operating bandwidth and increase the radiating aperture, a parasitic patch of dimensions W_2 and L_2 is placed on the parasitic layer on top of the radiating layer.

In order to obtain quad polarization, a switchable feeding network with three switchable probes P_1, P_2, and P_3 and three PIN diodes D_1, D_2, and D_3 are implemented on the feed network layer as shown in Fig. 4.1 (c). The polarization of the antenna element is independently controlled by switching the three probes. The whole antenna element performance is investigated and optimized through the simulation using the full wave electromagnetic solver, i.e., HFSS software [125]. The optimized design parameters are mentioned in the Table 4.1. To control the ON/OFF states of the PIN diodes, the DC biasing circuit is designed on the feed network layer itself so that it does not interfere with antenna radiation characteristics. In DC biasing, a lumped inductor (L) of 22 nH and a capacitor (C) of 6 pF are used to block the RF current and DC current, respectively. Besides, RF PIN diodes (BAR 64-02 V) from Infineon Technology [124] are modeled in the simulation process according to the equivalent circuit, as illustrated in Fig. 2.4.

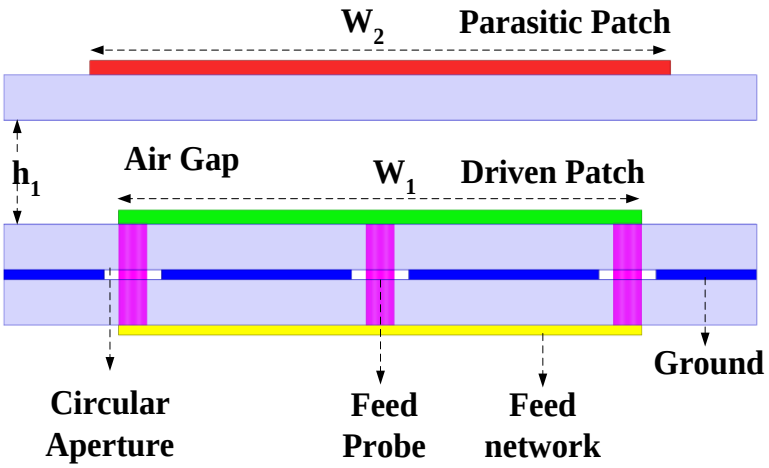

(a)

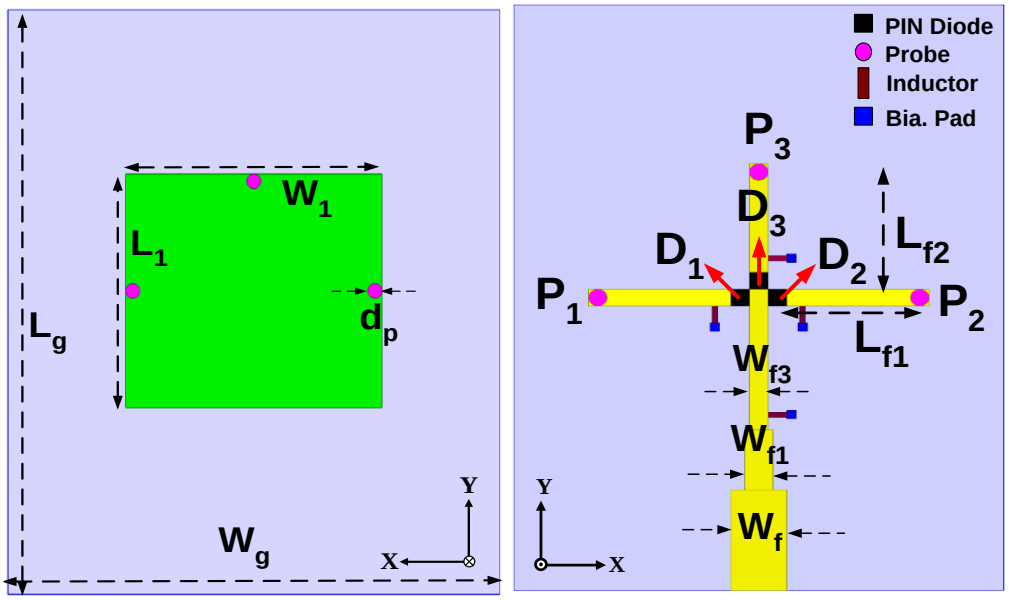

(b) (c)

Figure 4.1: Structure of the proposed reconfigurable array element. (a) side view. (b) driven patch layer. (c) feed network layer.

Further, to demonstrate the working principle, a step by step design procedure is summarized in Fig. 4.2. Initially, as shown in Fig. 4.2(a), a conventional microstrip patch antenna with narrow bandwidth and broadside radiation pattern is designed as case 1. Secondly, to enhance the operating bandwidth and antenna radiation aperture, a parasitic

Table 4.1: **Optimized dimensions of the antenna element**

Parameter	Value (mm)	Parameter	Value (mm)	Parameter	Value (mm)
W_1	18.24	W_g	35	W_{f2}	1
L_1	16	L_g	27	L_{f1}	7.62
W_2	20.24	d_P	1	L_{f2}	6.5
L_2	18	W_f	3		
h_1	5	W_{f1}	1.5		

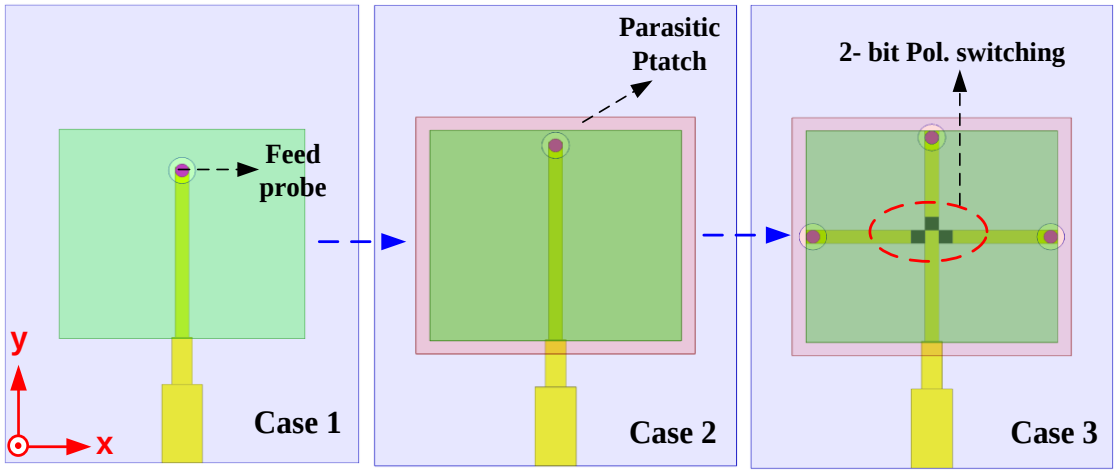

(a) (b) (c)

Figure 4.2: Design steps of the proposed reconfigurable element (a) single probe fed patch radiator, (b) parasitic patch loaded element, (c) 2-bit polarization reconfigurable element.

patch is loaded on the conventional patch antenna which is represented as case 2 (Fig. 4.2(b)). Fig. 4.3(a) represents the surface current distribution in case 1 and case 2. It is observed that case 2 realizes a more uniform current distribution on the whole patch as compared to case 1.

Finally, as shown in Fig. 4.2(c), the single feed probe structure is replaced by a three-switch loaded triple feed probe structure (case 3) to obtain quad polarization switching. The

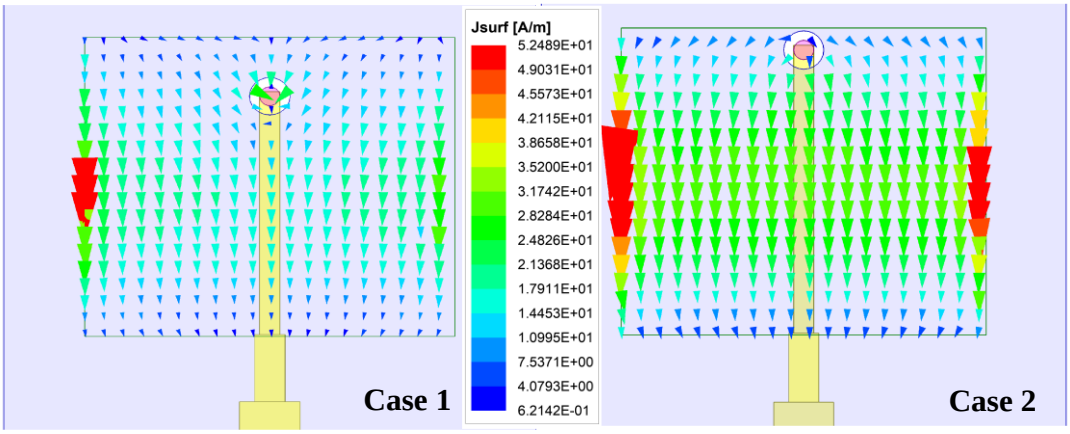

(a)

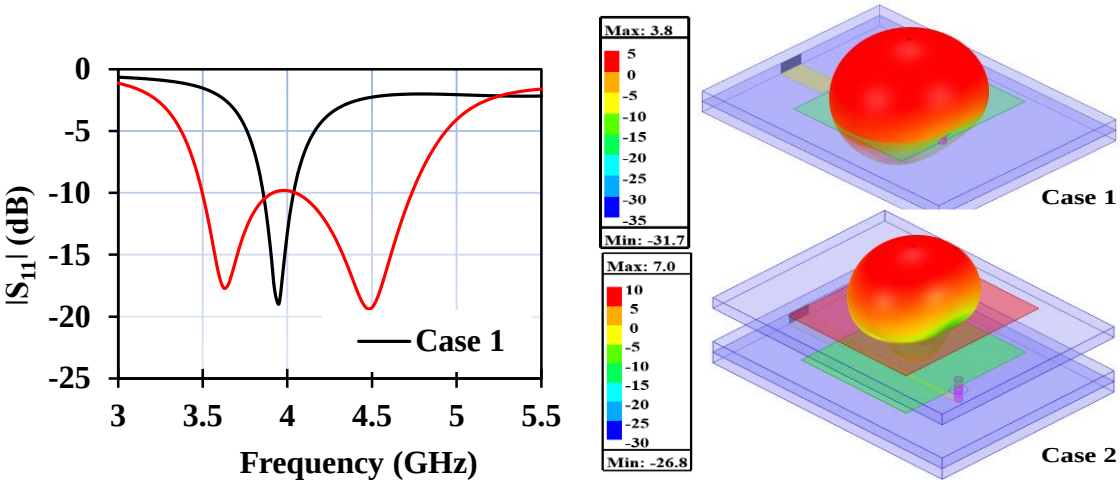

(b) (c)

Figure 4.3: Simulated results of the proposed antenna element with the parasitic patch (Case 2) or without parasitic patch (Case 1) (a) surface current distribution, (b) reflection coefficient and (c) radiation directivity.

corresponding simulated S_{11} and AR in case 3 with different polarization states are shown in Fig 4.4. It can be observed that the results are consistent due to the antenna's symmetrical structure. The simulated bandwidths for S_{11} < - 10 dB and AR < 3 dB range from 3.65-4.75 GHz and 3.6-4.05 GHz, respectively.

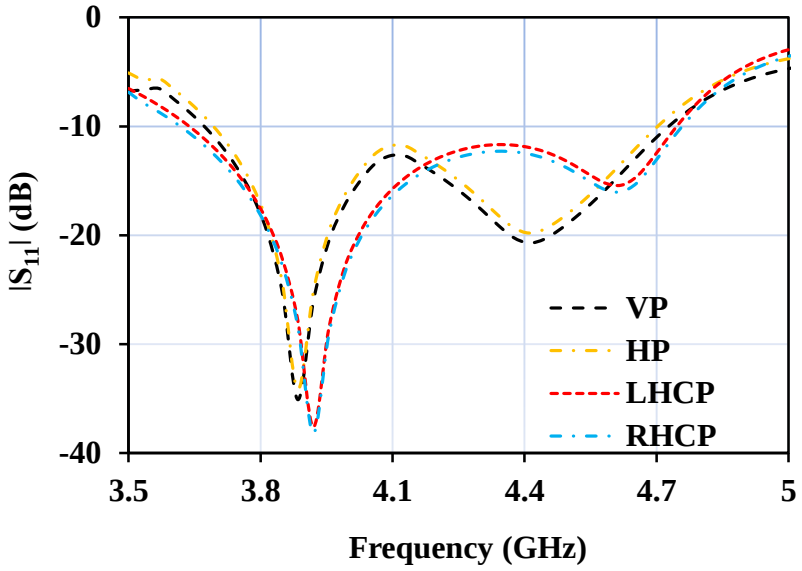

(a)

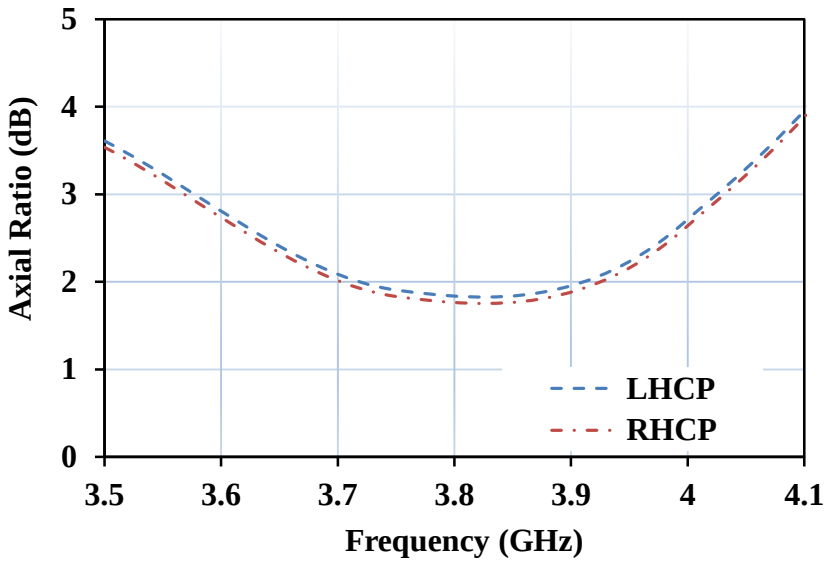

(b)

Figure 4.4: Simulated results of the array element with different exciting probes and corresponding polarization states. (a) reflection coefficient. (b) axial ratio.

To further understand the operating principle of the polarization reconfigurability, the simulated vector surface current distribution at 4.2 GHz for four different polarization states is mentioned in Fig. 4.5. In the VP state, both the diodes D_1 and D_2 are switched off to disconnect the probe P_2 and P_3 from the driven patch. In this case, the driven patch is

connected to the probe P_3, and a Y-directed surface current distribution is observed, as verified in Fig. 4.5 (a).

In the HP state, when probes P_1/P_2 are connected to the patch through diodes D_1/D_2, an X- polarized radiation wave is excited. For generating circular polarization (CP), the

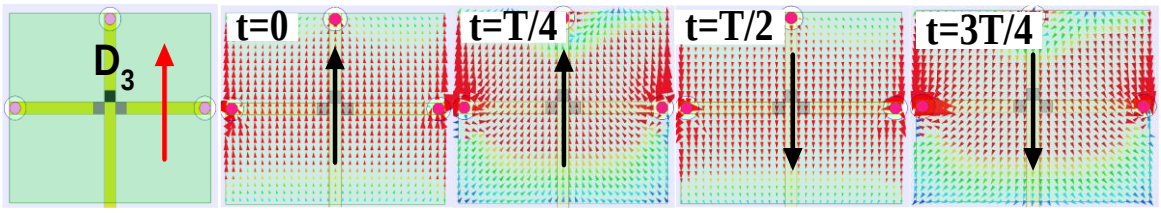

(a)

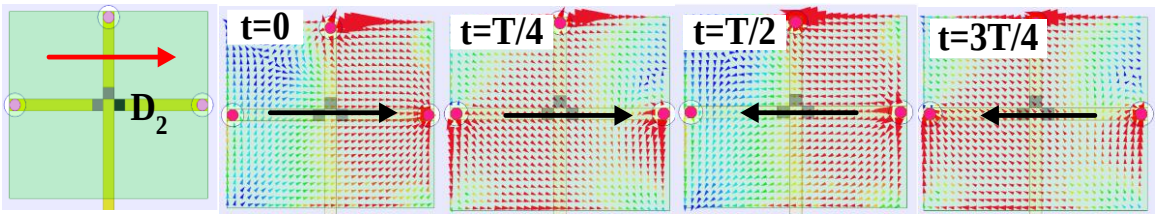

(b)

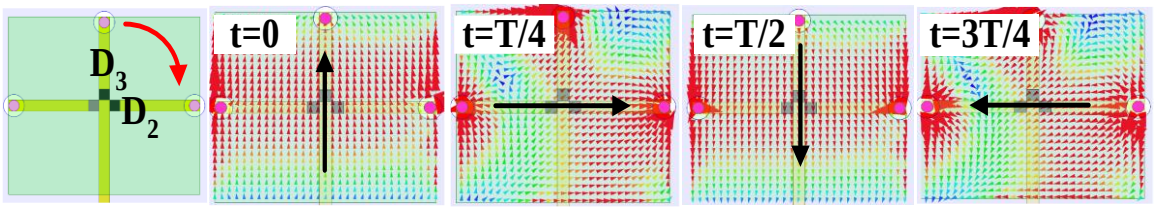

(c)

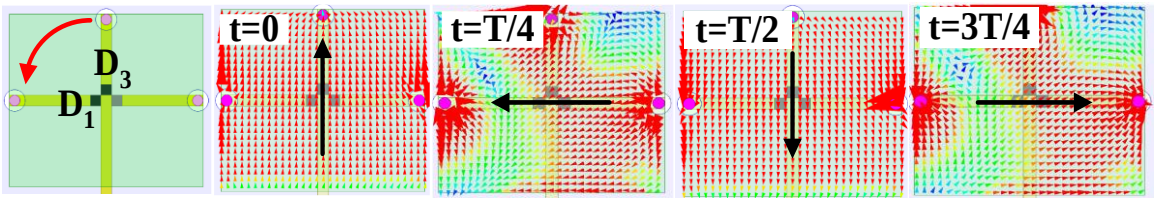

(d)

Figure 4.5: Simulated vector surface current distribution of the array element in four different polarization states. (a) VP (b) LP (c) LHCP (d) RHCP.

Table 4.2: **PIN diode biasing conditions and coding scheme for different polarization states**

D_1	D_2	D_3	Code	Polarization
OFF	OFF	ON	00	VP
OFF (ON)	ON(OFF)	OFF	01	HP
OFF	ON	ON	10	LHCP
ON	OFF	ON	11	RHCP

combination of the two orthogonal probes, P_1 P_3 or P_2 P_3 is selected. Due to the spatial relative position between the three feeding probes P_1, P_2 and P_3, the combination of probe excitation (P_1 P_3 or P_2 P_3) at three feed probes can obtain the 90° phase difference with equal amplitude required for CP generation [83]. For example, in the case when diode D_2, D_3 is switched ON, and D_1 is switched OFF, the vector current rotates in a clockwise sense with the increase in the time phase, which indicates that the antenna works in the LHCP state. Similarly, when diode D_2 is switched OFF, and D_1, D_3 is switched ON, the vector states of the currents rotate in opposite sense, generating RHCP as confirmed in Fig. 4.5(c). In brief, by changing the states of three PIN diodes, the proposed reconfigurable element can realize 2-bit quad-polarization switching. Table 4.2 represents the relationship between the different polarization and their corresponding coding sequence. Here, the four polarization states are coded as VP-00, HP-01, LHCP-10, and RHCP-11.

4.2.2 Design of 2×2 Pattern and Polarization Reconfigurable Array

Based on the proposed quad polarization reconfigurable antenna element, a 2×2 pattern and polarization reconfigurable array antenna having the potential to reconfigure its polarization and radiation pattern is developed. The proposed pattern and polarization reconfigurable array antenna consists of four stacked driven and parasitic patches separated by 0.6 λ_0 and a feed network comprising of PIN diodes and DC biasing circuit as shown in Fig. 4.6. The total volume of the proposed array antenna is 1.6 λ_0 × 1.6 λ_0 × 0.1 λ_0.

To obtain the beam steering operation, a 2-bit phase shifter designed in Chapter 2 (Fig.2.3) is integrated with a 2-bit polarization tuner (Fig. 4.1) discussed in section 4.2.1, as illustrated in Fig. 4.7(a). The zoomed-in view of the 2-bit phase shifter is shown in Fig. 4.7 (b). The feed network, including the DC biasing circuit, is implemented on the bottom side of the grounded substrate.

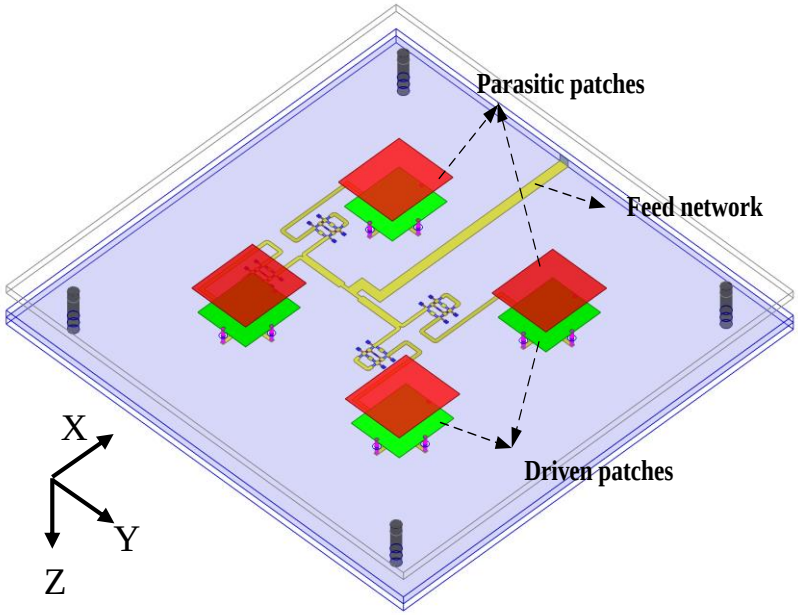

(a)

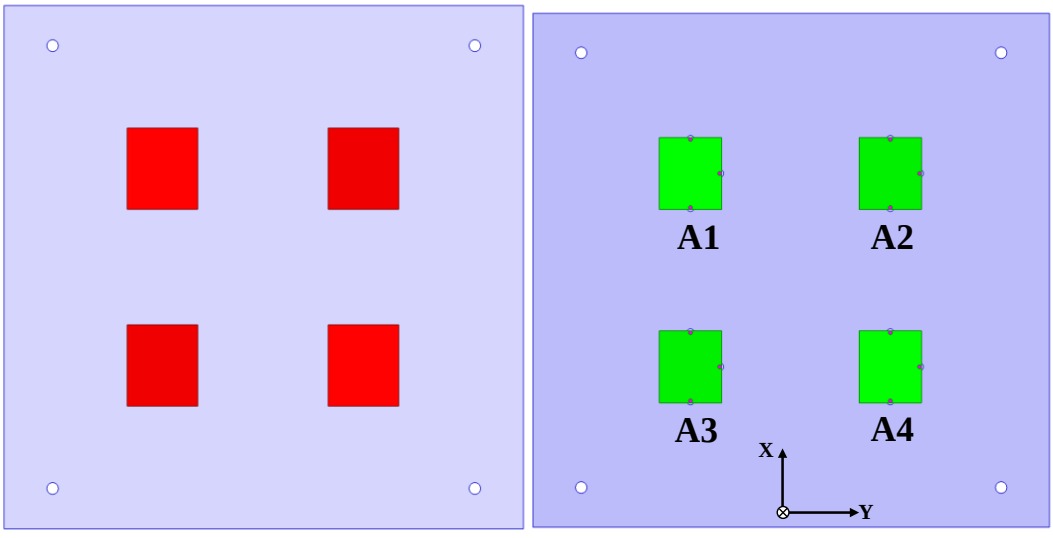

(b) (c)

Figure 4.6: Schematic of the proposed polarization and 2-D beam steering antenna array (a) isometric view (b) parasitic patch layer (c) driven patch layer.

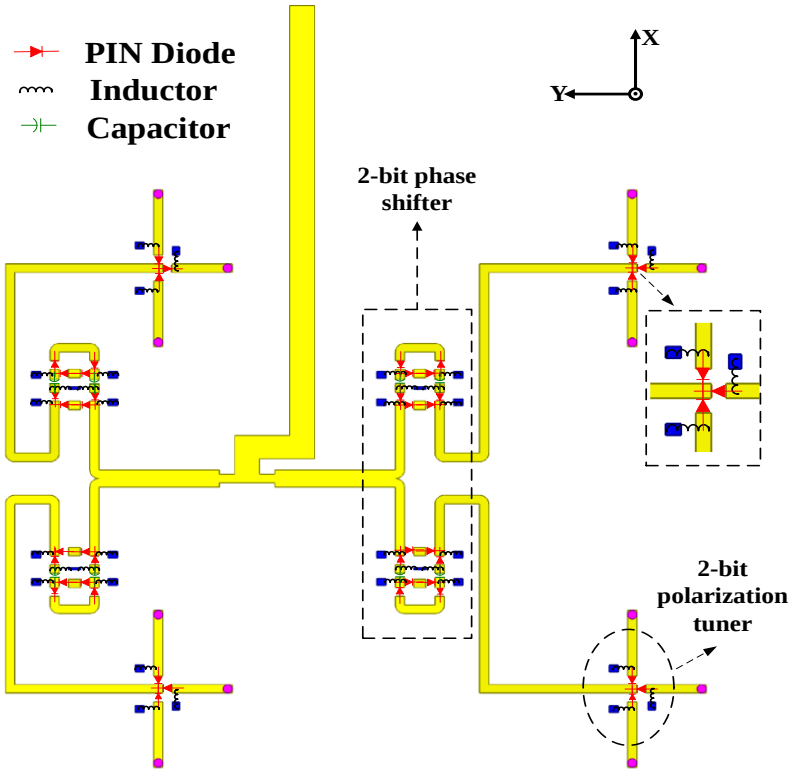

(a)

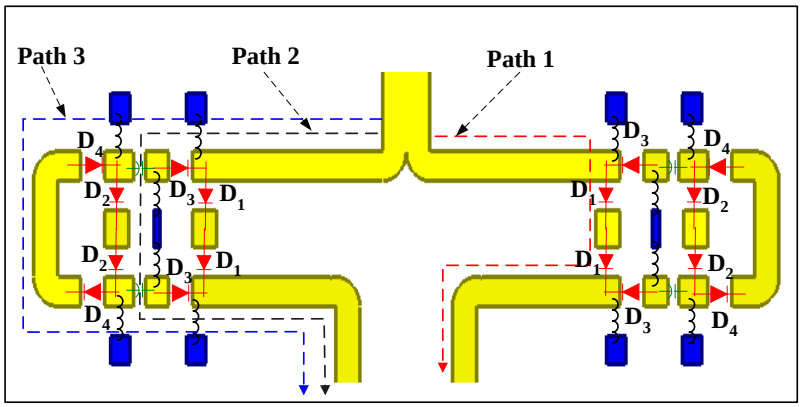

(b)

Figure 4.7: (a) Designed feed network of the proposed polarization and 2-D beam switchable antenna array (b) zoomed-in view of the 2-bit phase shifter.

4.2.3 Pattern Reconfiguration Implementation and Operating Principle

To understand the principle of pattern reconfiguration and explore the application potential of the proposed antenna array, the proposed polarization and beam steering using binary coding method is studied. The four driven antenna elements are denoted as A1-A4, shown in Fig. 4.6(b). For beam steering operation, each element of the array antenna is fed through

three different switchable feeding paths (Path 1 - Path 3) connected through diodes D_1-D_4, as shown in the zoomed view (Fig. 4.7(b)). Each path is represented in three different colours, red for path 1, black for path 2 and blue for path 3 (Fig. 4.7(b)), When the antenna array is excited through path 1, diode D1 is turned ON while other diodes are kept in OFF state. Similarly, for path 2, diodes D2 and D3 are turned ON and other diodes are turned OFF and for path 3 diodes D2 and D4 are turned ON and rest are in OFF states.

The different excitation phases at each array element provided by the three switchable feeding paths are represented in 2-bit binary codes. By controlling the ON-OFF combination of the four PIN diodes (D_1-D_4) on the feed paths, a broadside and various tilted beams are realized. Table 4.3 represents the states of the PIN diodes for three different feeding branches and their coding sequences of the proposed 2-bit phase shifter. Here, path 1 through diode D_1 is presented as "00", path 2 through diodes D_2 and D_3 are represented as "01", and path 3 through diodes D_3 and D_4 are coded as "10".

After design of the 2-bit polarization tuner and 2-bit phase shifter, a 2×2 array antenna is developed. Firstly, the polarization of each element is selected by choosing the coding sequence of the 2-bit polarization tuner ("00", or "01", or "10", or "11"). After selecting the polarization, the input excitation phase of every element is controlled by a 2-bit phase shifter ("00", or "01", or "10"). Based on the proposed concept, the proposed reconfigurable array can realize thirty-six (36) different radiation modes. The switching states of each element in different realized modes, along with coding sequences, are summarized in Table 4.4. There are four polarization states and nine beam steering states which are denoted as S_{11}-S_{19}, S_{21}-S_{29}, S_{31}-S_{39}, and S_{41}-S_{49} as shown in Table 4.4, where first subscript denotes polarization states and second subscript denotes the beam steering states. In Table 4.4, the first two bits are used to represent the input excitation phase at each array element and the last two binary bits are used to determine the different polarization

types on each element. Thus modes S_{11}-S_{19}, S_{21}-S_{29}, S_{31}-S_{39} and S_{41}-S_{49} represents nine different beam directions for VP, HP, LHCP and RHCP respectively.

Table 4.3: **PIN diode biasing conditions and their coding for different feeding paths**

D_1	D_2	D_3	D_4	Phase coding	Feeding branch
ON	OFF	OFF	OFF	00	Path 1
OFF	ON	ON	OFF	01	Path 2
OFF	OFF	ON	ON	10	Path 3

Table 4.4: **Coding schemes in different polarization and phase controlling modes of array antenna**

Mode	A1	A2	A3	A4	Mode	A1	A2	A3	A4	Description
S_{11}	0000	0000	0000	0000	S_{31}	0010	0010	0010	0010	Broadside
S_{12}	0000	0100	0100	0000	S_{32}	0010	0110	0110	0010	Tilted front in XZ plane
S_{13}	0000	1000	1000	0000	S_{33}	0010	1010	1010	0010	
S_{14}	0100	0000	0000	0100	S_{34}	0110	0010	0010	0110	Tilted back in XZ plane
S_{15}	1000	0000	0000	1000	S_{35}	1010	0010	0010	1010	
S_{16}	0100	0100	0000	0000	S_{36}	0110	0110	0010	0010	Tilted front in YZ plane
S_{17}	1000	1000	0000	0000	S_{37}	1010	1010	0010	0010	
S_{18}	0000	0000	0100	0100	S_{38}	0010	0010	0110	0110	Tilted back in YZ plane
S_{19}	0000	0000	1000	1000	S_{39}	0010	0010	1010	1010	
S_{21}	0001	0001	0001	0001	S_{41}	0011	0011	0011	0011	Broadside
S_{22}	0001	0101	0101	0001	S_{42}	0011	0111	0111	0011	Tilted front in XZ plane
S_{23}	0001	1001	1001	0001	S_{43}	0011	1011	1011	0011	
S_{24}	0101	0001	0001	0101	S_{44}	0111	0011	0011	0111	Tilted back in XZ plane
S_{25}	1001	0001	0001	1001	S_{45}	1011	0011	0011	1011	
S_{26}	0101	0101	0001	0001	S_{46}	0111	0111	0011	0011	Tilted front in YZ plane
S_{27}	1001	1001	0001	0001	S_{47}	1011	1011	0011	0011	
S_{28}	0001	0001	0101	0101	S_{48}	0011	0011	0111	0111	Tilted back in YZ plane
S_{29}	0001	0001	1001	1001	S_{49}	0011	0011	1011	1011	

4.3 Results and Discussion

To verify the radiation characteristics of the proposed four-element planar array is fabricated as depicted in Fig. 4.8. Due to symmetry in the realized polarization, the experimental measurement is carried out only for VP modes (S_{11}-S_{17}) and RHCP modes (S_{41}-S_{47}). The reflection coefficients of the proposed 2-D beam steerable antenna in different coding states for VP ($S_{11/12/13/14/15/16/17}$) and RHCP ($S_{41/42/43/44/45/46/47}$) are measured using the Anritsu VNA Master MS2038C. Fig. 4.9 and Fig. 4.10 represent the simulated and measured results in VP and RHCP modes for different beam switching states, respectively. An overlapped –10 dB impedance bandwidth of 29.2% ranging from 3.5 GHz to 4.7 GHz is observed for both VP and RHCP modes.

Far field radiation characteristics of the antenna are measured in the anechoic chamber where the phase and magnitude of the far field component E_θ and H_ϕ are measured to evaluate the axial ratio using the equations 3.1–3.3.

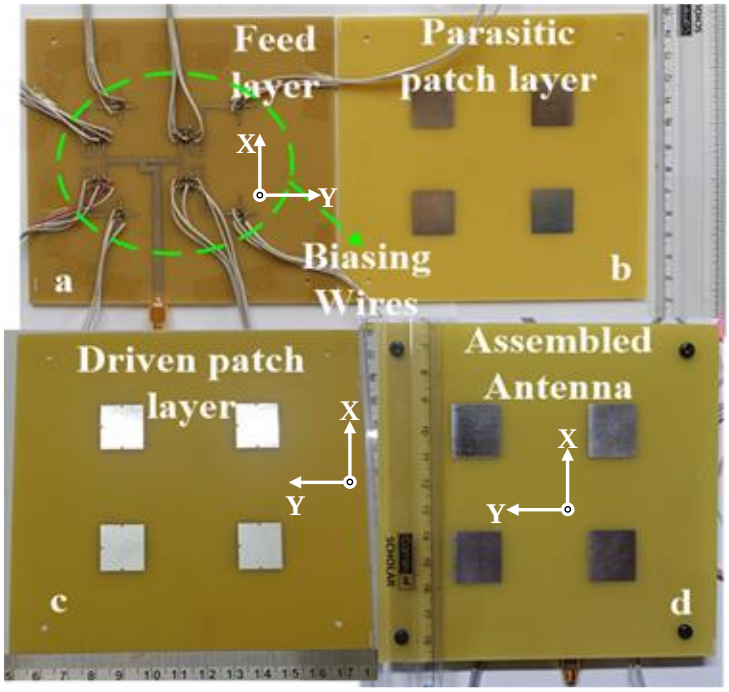

Figure 4.8: Fabricated prototype of the proposed antenna (a) feed layer (b) parasitic layer (c) driven patch layer (d) assembled antenna.

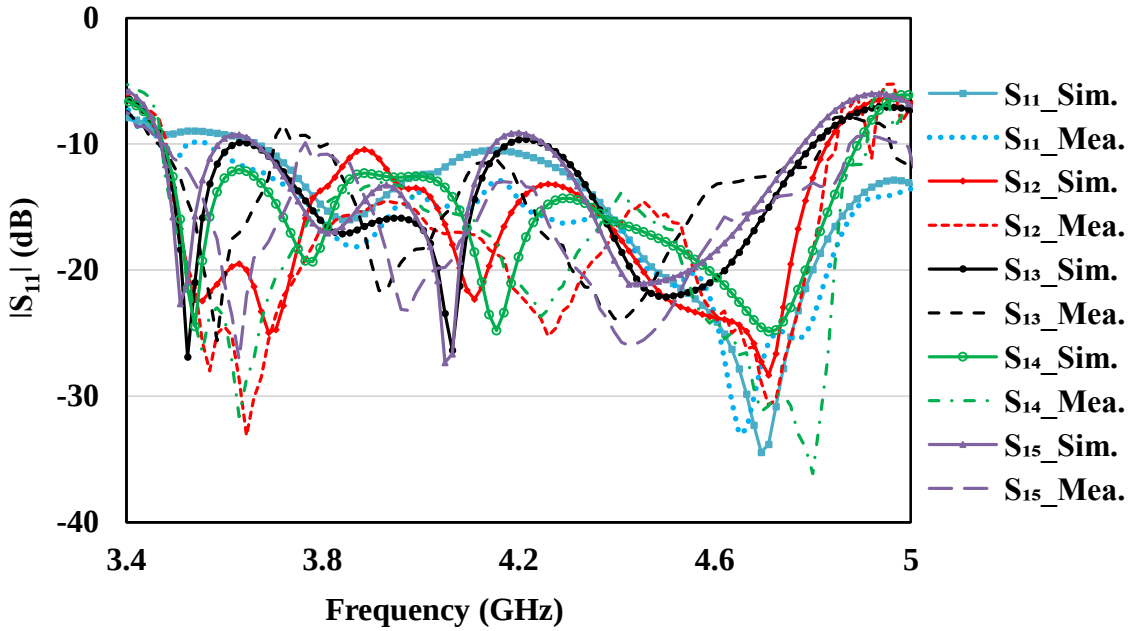

(a)

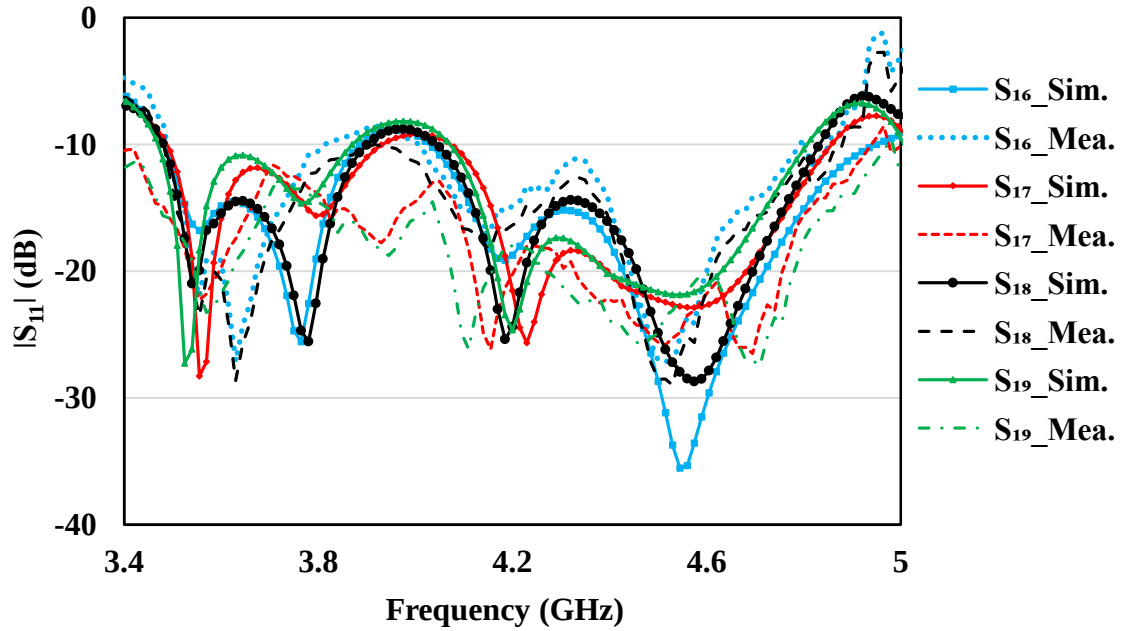

(b)

Figure 4.9: Simulated and measured S-parameters in VP state. (a) XZ Plane and (b) YZ Plane.

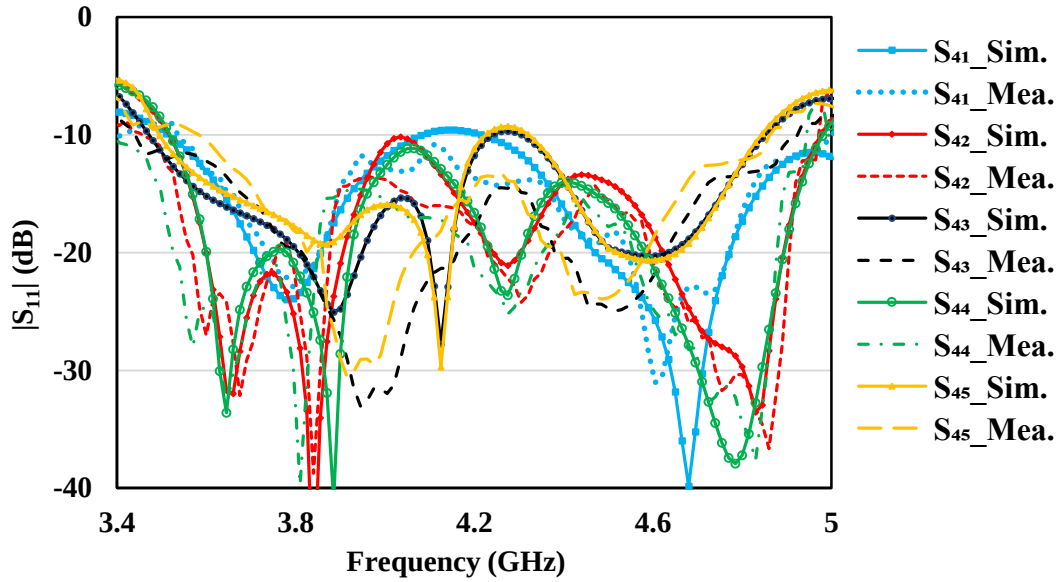

(a)

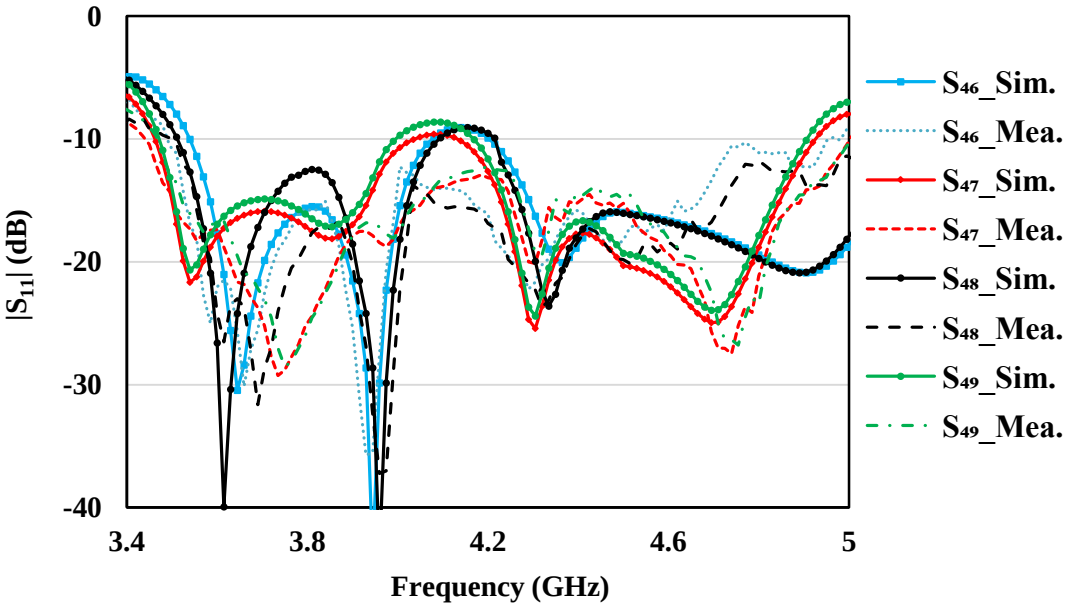

(b)

Figure 4.10: Simulated and measured S-parameters in RHCP state. (a) XZ Plane and (b) YZ Plane.

The measured and simulated axial ratio of the antenna at the maximum radiation direction is depicted in Fig. 4.11, where simulation results are also included for comparison. A good agreement between simulated and measured results is observed. The measured 3-dB axial

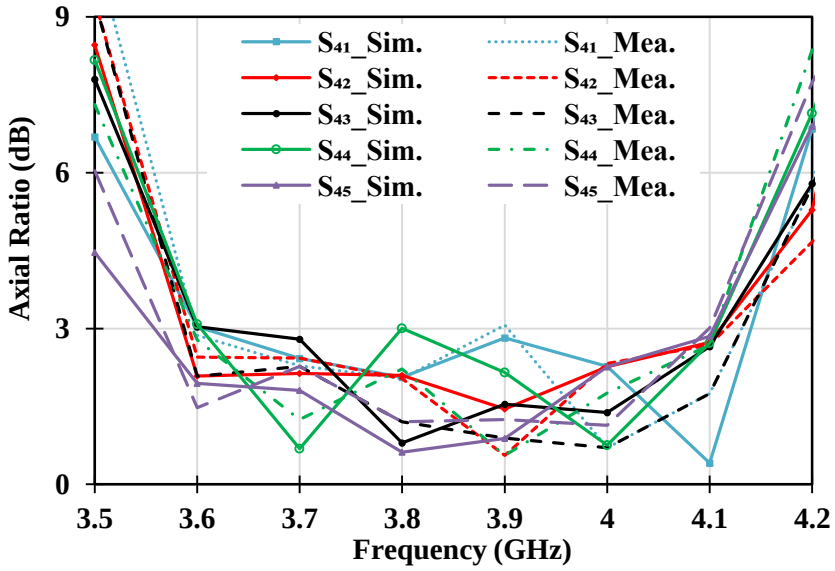

(a)

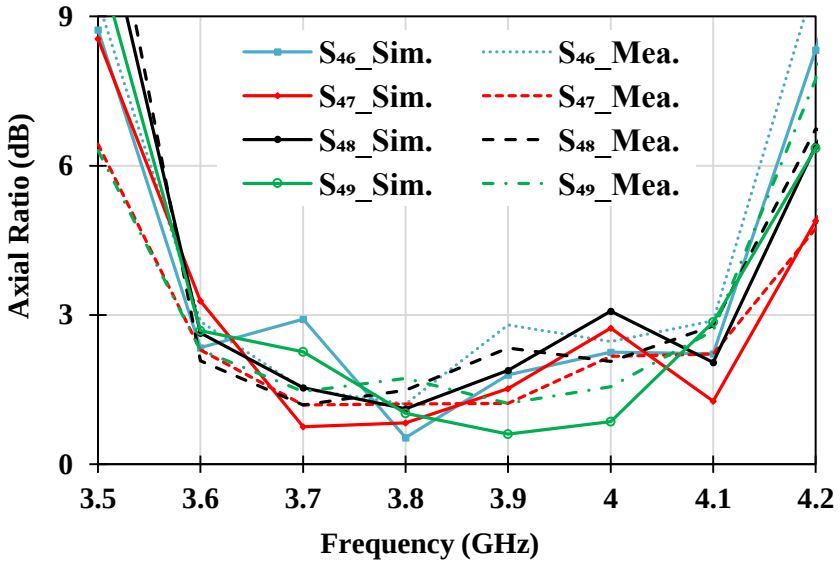

(b)

Figure 4.11: Measured and simulated axial ratios in RHCP. (a) XZ plane and (b) YZ plane.

ratio bandwidth in both the XZ-plane and YZ-plane can cover a frequency range from 3.6 GHz to 4.2 GHz and 3.6 GHz to 4.1 GHz, respectively for all realized modes.

The simulated and measured gain for VP and RHCP modes are compared in Fig. 4.12. As observed from Fig. 4.12, the gain for nine beams switching states in XZ plane and YZ plane varies from 11.02 dBi to 7 dBi and 11.07 dBi to 7.2 dBi for VP and RHCP modes, respectively.

The normalized simulated and measured far field radiation patterns of the 2-D beam steering planar array are shown in Fig. 4.13 and Fig. 4.14 for VP and RHCP, respectively. It is observed from Fig. 4.13(a-e), for VP modes, the main beam of the proposed array can steer up to ±28° in the both XZ and YZ planes. A similar beam steering performance is observed for RHCP mode also as presented in Fig. 4.14(a-e).

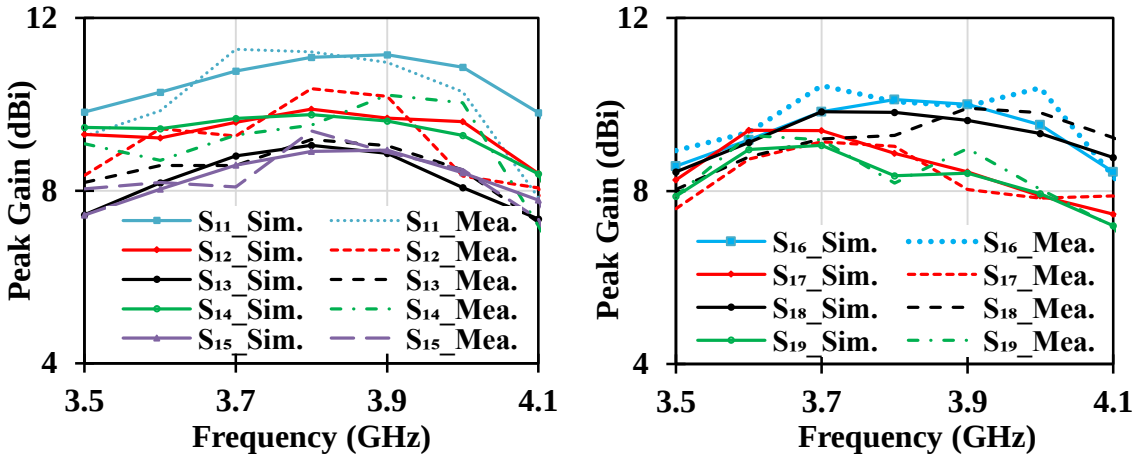

(a)

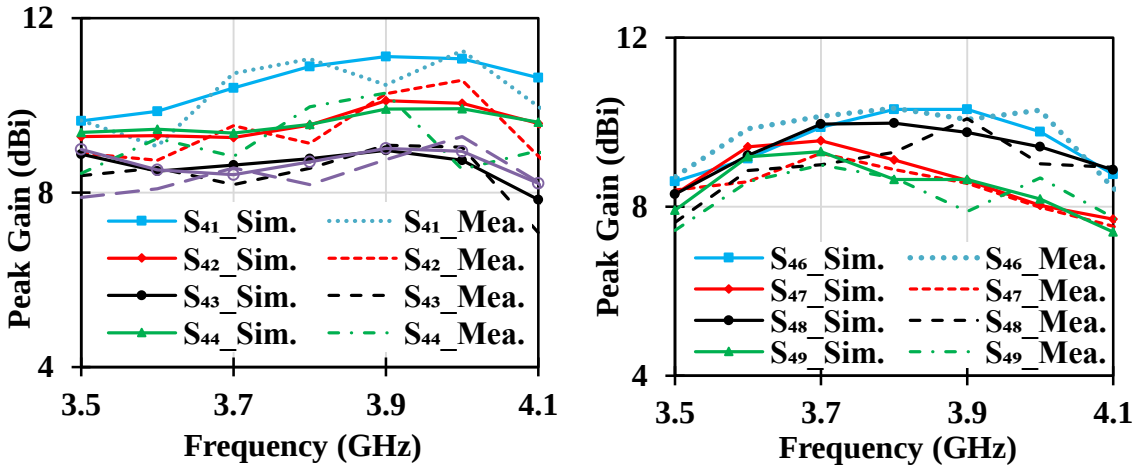

(b)

Figure 4.12: Measured and simulated gain in (a) VP mode and (b) RHCP mode.

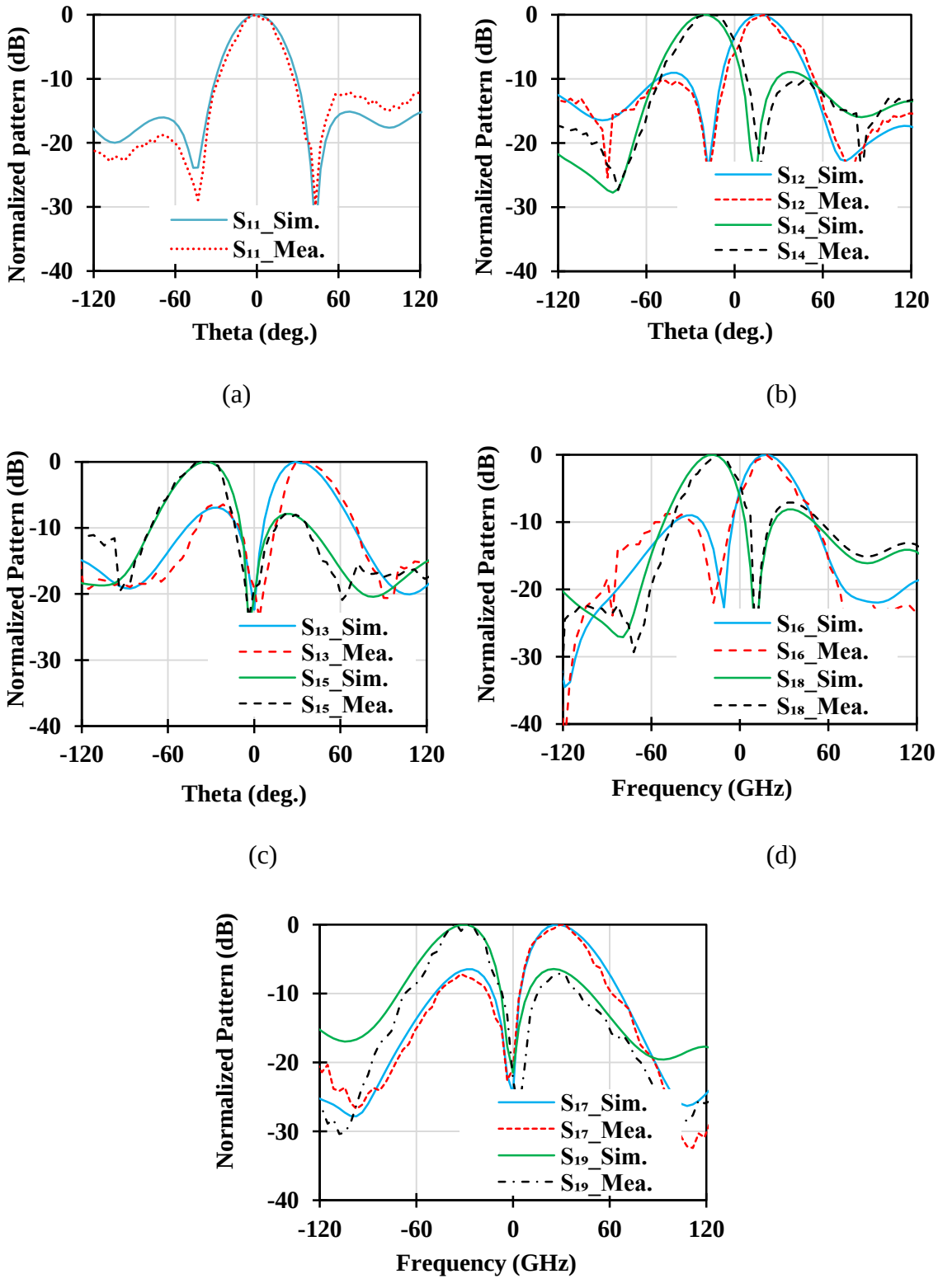

Figure 4.13: Measured and simulated normalized radiation patterns VP mode. (a), (b) XZ Plane and (c) YZ Plane.

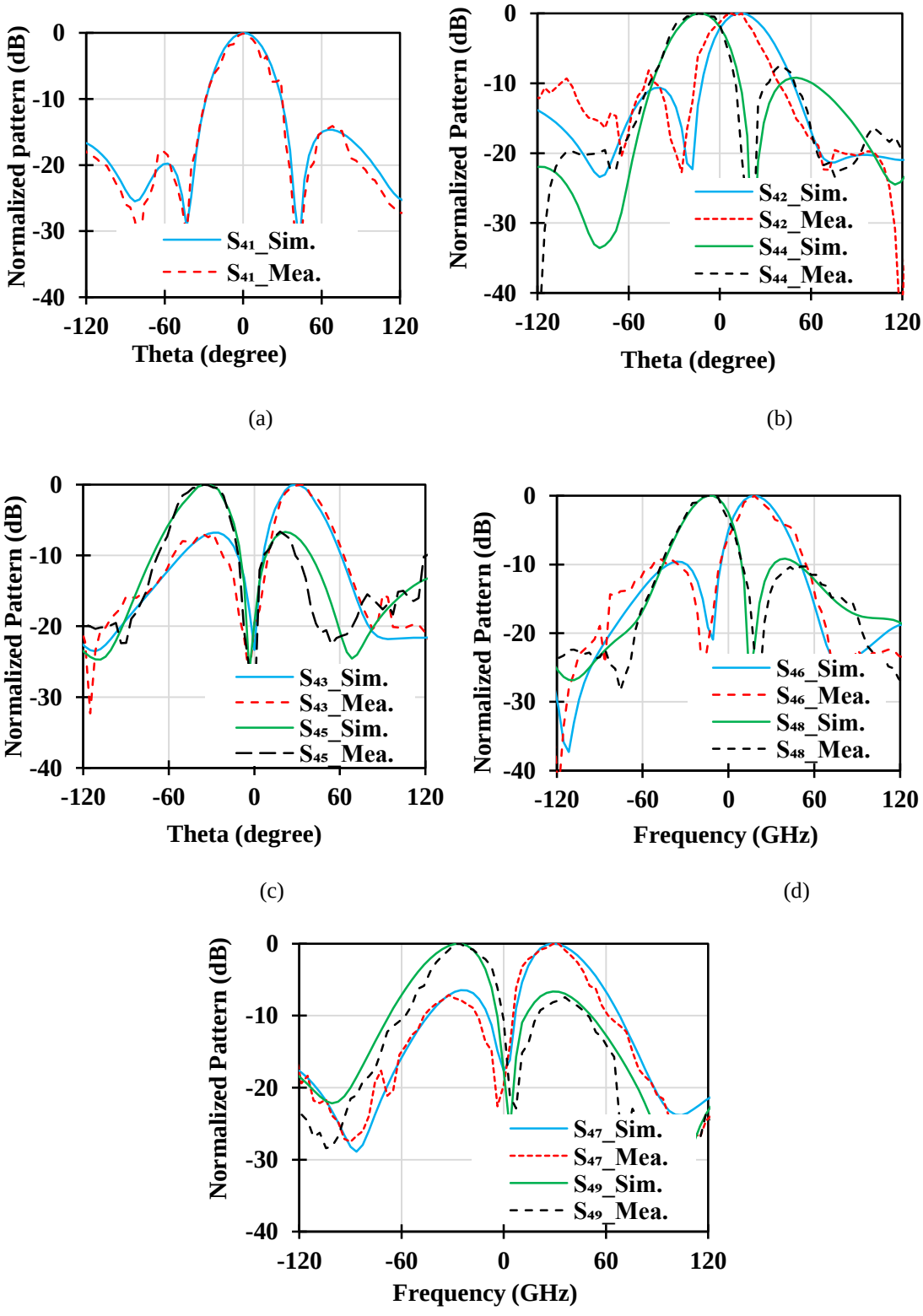

Figure 4.14: Measured and simulated normalized radiation pattern RHCP mode. (a), (b), (c) XZ Plane and (d), (e) YZ Plane.

4.4 Comparison and Review

To further explain the novelty and advantages of the proposed design, a performance comparison with the existing similar literature have been summarized in Table 4.5. A dual circularly polarized antenna with 1-D beam steering was realized in ref [83], [154] and [144]. Ref. [154] realizes wide impedance and AR bandwidth with two polarization states have been reconfigured. Antenna reported in [145] has three polarization states but their complex multipath control system limits their practical application. Ref. [155] and [156] proposed an array with quad polarization states and 1-D beam steering but their impedance and axial ratio

bandwidth is very narrow. Compared with the existing work the advantages of the proposed design can be summarized as:

1). The proposed design shows wider IMBW among all except in [145] and wider 3 dB ARBW except in [154] and [145].

2). The proposed antenna realizes a 2-D beam steering with four polarization states. As per the authors' knowledge such kind of reconfigurability is not available in the literature.

3). Additionally, the proposed design realizes wider impedance bandwidth and 3 dB axial ratio bandwidth using a simple and low cost structure.

4.5 Summary

A 2×2 planar array antenna with quad polarization states and 2-D beam switching is developed and studied. A new pattern and polarization coding mechanism is proposed to achieve 2-bit polarization states and 2-bit phase states. By exploring the polarization tuner and transmission line based phase shifter, the proposed array can realize 2-D beam steering from –28° to +28° in both XZ and YZ plane with four polarization states including HP, VP, RHCP and LHCP. Finally, a four-element planar array with thirty-six radiation modes is designed fabricated and measured to validate the proposed digital coding concept. The

proposed antenna finds a good application in 5G sub-6GHz frequency band and in future beam steering intelligent systems.

Finally, the key findings, research contributions and concluding remarks of the presented research investigations are summarized in Chapter 5. An overview of future research work related to the presented research in this thesis is presented at the end of the chapter.

Table 4.5: **Comparison of the proposed beam steering antenna with the similar antenna**

Ref.	AT	P(λ_0)^3	PD	BS	IMBW	ARBW	R
[83]	2x2 PAA	1.6x1.6x 0.07	LHCP/RHCP	2-D	9	4.2	Narrow BW with dual polarization
[154]	1x2 PAA	1.04x1.0 4x0.19	LHCP/RHCP	1-D	23	17.4	Wide BW, Limited polarization states
[144]	1x4 PAA	0.85x2.3 4x0.05	LHCP/RHCP	1-D	14.7	8	High cost (larger no of diodes)
[145]	1x4 DAA	1.87x2.3 4x0.33	LP/LHCP/ RHCP	1-D	38.5	18	limited beam control capacity, complex structure
[155]	1x4 DRAA	0.64x1.9 5x0.08	VP, HP, LHCP, RHCP	1-D	12.5	2.4	Narrow ARBW, 1-D switching
[156]	1x4 I-VAA	2.9x3.58 x0.58	VP, HP, RHCP, LHCP	1-D	15.7	-	Large in size (dual butler matrix BFN), high cost
This Work	2x2 PAA	1.82x1.8 2x0.11	VP, HP, LHCP RHCP	2-D	29	13	Wide BW, 2D- beam switching with quad polarization states

Here AT = antenna type, P = profile, PD = polarization diversity, BS = beam switching, R = remarks, PAA = patch antenna Array, DAA = dipole Antenna array, DRAA = dielectric resonator antenna array, IVAA = inverted-V antenna array, IMBW = impedance bandwidth, ARBW = axial ratio bandwidth, BW = bandwidth, BFN = beam forming network